Benchmark on Discretization Schemes for Anisotropic Diffusion Problems on General Grids

Raphaèle Herbin and Florence Hubert

Laboratoire d'Analyse, Topologie et Probabilités, UMR 6632
Université de Marseille
39 rue Joliot Curie 13453 Marseille, France
herbin@cmi.univ-mrs.fr, fhubert@cmi.univ-mrs.fr

ABSTRACT. *We present here a number of test cases and meshes which were designed to form a benchmark for finite volume schemes and give a summary of some of the results which were presented by the participants to this benchmark. We address a two-dimensional anisotropic diffusion problem, which is discretized on general, possibly non-conforming meshes. In most cases, the diffusion tensor is taken to be anisotropic, and at times heterogeneous and/or discontinuous. The meshes are either triangular or quadrangular, and sometimes quite distorted. Several methods were tested, among which finite element, discontinous Galerkin, cell centred and vertex centred finite volume methods, discrete duality finite volume methods, mimetic methods. The results given by the participants to the benchmark range from the number of unknowns, the errors on the fluxes or the minimum and maximum values and energy, to the order of convergence (when available).*

KEYWORDS: *Anisotropic medium, diffusion process, finite volume schemes, benchmark*

1. Introduction

The aim of this benchmark is to provide a number of test cases in order to test the properties (convergence, robustness...) of existing discretization schemes for anisotropic diffusion problems using general grids. In all test cases except test 8, the domain Ω is the unit square. The boundary of the domain is divided into $\partial\Omega = \Gamma_D \cup \Gamma_N$ where Dirichlet (resp. Neumann) boundary conditions are given on Γ_D (resp. on Γ_N). The considered diffusion problem is formulated as:

$$- \quad \nabla\cdot(\mathbf{K}\nabla u) = f \text{ on } \Omega, \qquad [1]$$

$$u = \bar{u} \text{ on } \Gamma_D, \qquad [2]$$

$$\mathbf{K}\nabla u \cdot \mathbf{n} = g \text{ on } \Gamma_N, \qquad [3]$$

where $\mathbf{K} : \Omega \to \mathbb{R}^{2\times 2}$ is the diffusion (or permeability) tensor, f the source term, $\bar{u}$ and g the Dirichlet and Neumann boundary conditions, and $\mathbf{n}$ denotes the outward unit normal vector to Γ_N. For each test case, we propose some meshes which are used for the discretization of Problem [1] by the various schemes. These meshes are depicted in section 15 below.

2. The participating schemes and teams

Even though the benchmark is associated with the FVCA5 conference, the call for submission was by no means restricted to finite volume schemes, and indeed several types of schemes were submitted:

Cell centred schemes

• CMPFA: *Compact-stencil MPFA method for heterogeneous highly anisotropic second-order elliptic problems*, by S. Mundal, D. A. Di Pietro and I. Aavatsmark, [**?**].

• FVHYB: *A symmetric finite volume scheme for anisotropic heterogeneous second-order elliptic problems*, by L. Agelas and D. A. Di Pietro, [**?**].

• FVSYM: *Numerical results with two cell-centered finite volume schemes for heteregeneous anisotropic diffusion operators*, by C. Le Potier, [**?**].

• SUSHI-P or SUSHI-NP (which are cell centred in their full barycentric version): *SUSHI: A Scheme Using Stabilization and Hybrid Interfaces for anisotropic heterogeneous diffusion problems*, by R. Eymard, T. Gallouët and R. Herbin, [**?**].

Control volume finite element schemes

• CVFE: *Numerical simulation for the anisotropic benchmark by a vertex-centred finite volume method*, by M. Afif and B. Amaziane, [**?**].

Discontinous Galerkin schemes

• DG-C: *The Compact Discontinuous Galerkin Method for Elliptic Problems*, by A. Dedner and R. Klöfkorn, [**?**].

• DG-W: *A discontinuous Galerkin flux for anisotropic heterogeneous second-order elliptic problems*, by D. A. Di Pietro and A. Ern, [**?**].

Discrete duality finite volume schemes

• DDFV-BHU: *The DDFV "discrete duality finite volumes" and m-DDFV schemes*, by F. Boyer and F. Hubert, [**?**].

• DDFV-HER: *Numerical experiments with the DDFV method, F. Hermeline, [**?**].*

• DDFV-MNI: *Some MPFA methods of DDFV type*, by I. Moukouop Nguena and A. Njifenjou, [**?**].

• DDFV-OMN: *Tests with the Discrete Duality Finite Volume method*, by P. Omnes, [**?**].

Finite element schemes

• FEP1, FEP2, FEQ1, FEQ2: *A Galerkin Finite Element Solution*, by G. Ansanay-Alex, B. Piar and D. Vola, [**?**].

Lattice Boltzmann schemes

• LATTB *Using Lattice Boltzmann scheme for anisotropic diffusion problems*, by F. Dubois, P. Lallemand and M. M. Tekitek, [**?**].

Mixed or hybrid methods

• MFD-BLS: *Mimetic finite difference method*, by K. Lipnikov, [**?**].

• MFD-FHE: *Numerical investigation of a mimetic finite difference method*, by B. Flemisch and R. Helmig, [**?**].

• MFD-MAN: *The mimetic finite difference method*, by G. Manzini, [**?**].

• MFD-MAR: *A mimetic finite difference method*, S. Marnach, [**?**].

• MFE: Mixed finite element (Raviart Thomas) programmed by the benchmark organizers for lack of a submission.

• MFV: *Use of the mixed finite volume method*, by C. Chainais-Hillairet, J. Droniou and R. Eymard [**?**].

• SUSHI-P or SUSHI-NP (which are hybrid in their full hybrid version): *SUSHI: A Scheme Using Stabilization and Hybrid Interfaces for anisotropic heterogeneous diffusion problems*, by R. Eymard, T. Gallouët and R. Herbin, [**?**].

Nonlinear schemes

The schemes are nonlinear in order to ensure the positivity of the scheme (that is, if the right hand side is positive then the solution is positive) or the discrete maximum principle (that is, if the linear system stems from the discretization of an elliptic equation satisfying the maximum principle, then its solution is also bounded by the bounds of the continuous system).

• FVPMMD: *Numerical results with two cell-centered finite volume schemes for heteregeneous anisotropic diffusion operators*, by C. Le Potier, [**?**].

• NMFV: *Nonlinear monotone finite volume method*, by D. Svyatskiy, [**?**].

Of course, the above choice of categories is neither exhaustive nor unique. In fact, most of these categories intersect: schemes are not so easy to classify, and some schemes are known to be identical in special cases. We refer to the above-cited papers for the details of the schemes and their implementation. Our purpose is to give here a synthesis of the results presented by the participants and raise some questions on the future trends in this field of research.

3. Nature of the results and notations

Some of the output results are given for all tests, and others only for those tests for which we know of an analytical solution. Here are both lists.

3.1. *For all tests*

- `nunkw` number of unknowns
- `nnmat` number of non-zero terms in the matrix
- `sumflux` the discrete flux balance, that is: $\texttt{sumflux} = \texttt{flux0} + \texttt{flux1} + \texttt{fluy0} + \texttt{fluy1} - \texttt{sumf}$, where `flux0, flux1, fluy0, fluy1` are the outward numerical fluxes at the boundaries $x = 0$, $x = 1$, $y = 0$ and $y = 1$ (for instance `flux0` is an approximation of $-\int_{x=0} \mathbf{K}\nabla u \cdot \mathbf{n}\, ds$) and $\texttt{sumf} = \sum_{K\in\mathcal{T}} |K| f(x_K)$ where x_K denotes some point of the control volume K. Let us note that for vertex methods such as the finite element schemes FE or the CVFE scheme, the points x_K are the vertices of the mesh. For most cell centred schemes, x_K is chosen as the centre of gravity for most schemes. Some papers concerning DDFV schemes (DDFV-OMN, DDFV-BHU) report results for values at two different points, but we shall only present here the results with x_K the centre of gravity of the primal mesh.

The residual `sumflux` is a measure of the global conservativity of the scheme; hence, it is expected to be of the order of the machine precision for all schemes which are based on a local conservation of fluxes. In fact, it was very useful in debugging codes; however, for the sake of conciseness, we choose not to display its value here since it is indeed of the machine precision order for FV type schemes and of the mesh size order for purely Galerkin finite element type schemes (FE).

- `umin`: value of the minimum of the approximate solution.
- `umax`: value of the maximum of the approximate solution.
- `ener1, ener2`, where `ener1` and `ener2` are approximations of the energy following the two expressions (which are identical in the continuous setting): `ener1, ener2`

$$E_1 = \int_\Omega \mathbf{K}\nabla u \cdot \nabla u dx,\ E_2 = \int_{\partial\Omega} \mathbf{K}\nabla u \cdot \mathbf{n}\, u dx \qquad [4]$$

Even though E_1 and E_2 converge to the same value on fine grids, there can be a noticeable difference between E_1 and E_2 on the coarsest meshes. Note also that we get an upper bound of the continuous value $E_1 = E_2$ by using a conformal finite element method and lower bound with the mixed finite element (Raviart–Thomas) method.

3.2. *When the analytical solution is known and the mesh refined*

Let us denote by u the exact solution, by $\mathcal{T}$ the mesh and by $u_\mathcal{T} = (u_K)_{K\in\mathcal{T}}$ the piecewise constant approximate solution.

- `erl2`, relative discrete L^2 norm of the error, for instance:

$$\texttt{erl2} = \left(\frac{\sum_{K\in\mathcal{T}} |K|(u(x_K) - u_K)^2}{\sum_{K\in\mathcal{T}} |K| u(x_K)^2} \right)^{\frac{1}{2}}.$$

• `ergrad` relative L^2 norm of the error on the gradient, if available

• `ratiol2`: for $\mathtt{i} \geq 2$,

$$\mathtt{ratiol2(i)} = -2\frac{\ln(\mathtt{erl2(i)}) - \ln(\mathtt{erl2(i-1)})}{\ln(\mathtt{nunkw(i)}) - \ln(\mathtt{nunkw(i-1)})}$$

• `ratiograd`, for $\mathtt{i} \geq 2$, same formula as above with `ergrad` instead of `erl2`.

• `erflx0,erflx1, erfly0,erfly1` relative error between `flux0, flux1, fluy0, fluy1` and the corresponding flux of the exact solution:

$$\mathtt{erflx0} = \left| \frac{\mathtt{flux0} + \int_{x=0} \mathbf{K}\nabla u \cdot \mathbf{n}}{\int_{x=0} \mathbf{K}\nabla u \cdot \mathbf{n}} \right|$$

(except for the fluxes at y=0 and y=1 for case test 2 - numerical locking - because these are zero).

• `erflm` L^∞ norm of the error on the meanvalue of the flux through the edges of the mesh, if available (give the definition of numerical flux $(\mathbf{K}\nabla u \cdot \mathbf{n})_{\mathcal{T}}$)

$$\mathtt{erflm} = \max\left\{ \left| \frac{1}{|\sigma|} \int_\sigma (\mathbf{K}\nabla u \cdot \mathbf{n} - (\mathbf{K}\nabla u \cdot \mathbf{n})_{\mathcal{T}}) \right|, \sigma \text{ edges of } \mathcal{T} \right\}.$$

• `ocvl2` order of convergence of the method in the L^2 norm of the solution as defined by `errl2` with respect to the mesh size:

$$\mathtt{ocvl2} = \frac{\ln(\mathtt{erl2(imax)}) - \ln(\mathtt{erl2(imax-1)})}{\ln(\mathtt{h(imax)}) - \ln(\mathtt{h(imax-1)})}$$

where `h` is the maximum of the diameter of the control volume.

• `ocvgradl2` order of convergence of the method in the L^2 norm of the gradient as defined by `ergradl2` with respect to the mesh size, same formula as above with `ergrad` instead of `erl2`.

4. Test 1: mild anisotropy

A homogeneous anisotropic tensor is first considered: $\mathbf{K} = \begin{pmatrix} 1.5 & 0.5 \\ 0.5 & 1.5 \end{pmatrix}$.

4.1. *Test 1.1: smooth solution,* `mesh1` *(triangular mesh) and* `mesh4` *(distorted quadrangular mesh)*

In this first test, we consider a very regular solution: $u(x,y) = 16x(1-x)y(1-y)$, we set $f = -\nabla \cdot (\mathbf{K}\nabla u)$, and we consider Dirichlet boundary conditions: $\Gamma_D = \partial\Omega$, $\Gamma_N = \emptyset$, and $\bar{u} = u|_{\partial\Omega}$. The schemes were first tested on a series of "regular" triangular meshes: `mesh1`, a picture of which is given in Figure 13. We give in Figure 1 the L^2 norm of the error versus the number of unknowns (upper left), the square root of the number of non zero matrix terms (upper right) and the step size `h` (lower left)

for all schemes for meshes `mesh1`. As can be seen on Figure 1, all schemes show an order 2 convergence except for the two higher order schemes FEP2 and DG-C, which are order 3. The schemes DDFV-HER, FEP2 and DG-C (see Figure 2) have an order 2 convergence with respect to the L^2 norm of the gradient; all other schemes show an order 1 convergence.

Note that when calculating the error with respect to `nunknw` and `nnmat`, the order of convergence remains the same (as expected) but the relative position of the schemes vary, as may be seen on the graphs of Figure 1. The behaviour or the L^2 norm of the gradient with respect to the three previous variables is depicted in Figure 2.

The same test was then carried out on two distorted quadrangular meshes `mesh4_1` and `mesh4_2` depicted in Figure 15. From Table 1 below, we can see that almost all schemes satisfy the discrete maximum principle on this test and meshes. The DG schemes DG-C and DG-W provide small negative values while the nonlinear (positive) scheme NMFV exceeds the maximum value 1. Note that some schemes include the boundary conditions in the calculation of the minimum and maximum values and others not. In the second case, if these minimum and maximum values are not equal to the boundary conditions, they can be taken as a measure of the accuracy of the scheme.

4.2. *Test 1.2:* `mesh1` *(triangular mesh) and* `mesh3` *(locally refined non-conforming rectangular mesh)*

We consider here the following exact solution: $u(x,y) = \sin\left((1-x)(1-y)\right) + (1-x)^3(1-y)^2$, with the right hand side $f = -\nabla \cdot (\mathbf{K}\nabla u)$, boundary conditions ($\Gamma_D = \partial\Omega$, $\Gamma_N = \emptyset$) and $\bar{u} = u|_{\partial\Omega}$. We use both the triangular mesh `mesh1` and the locally refined non-conforming rectangular mesh `mesh3`, which is depicted in Figure 14. The L^2 norm of the error and the gradient with respect with `nunknw`, `nnmat` and `h` are given in Figures 3 and 4 for the triangular mesh `mesh1` and, in Figures 5 and 6 for the locally refined non-conforming rectangular mesh `mesh3`.

As can be seen on Figure 3, the orders of convergence of the schemes are the same as in the case of Test 1.1. Similar results are observed on the locally refined non–conforming rectangular mesh `mesh3`.

Note from Figures 2, 4 and 6 that the L^2 norm of the gradient error is lower with the DDFV schemes than for the other second order schemes.

5. Test 2: Numerical locking [?, ?]

In this test, the permeability tensor is defined by:

$$\mathbf{K} = \begin{pmatrix} 1 & 0 \\ 0 & \delta \end{pmatrix}, \text{ with } \delta = 10^5 \text{ or } 10^6.$$

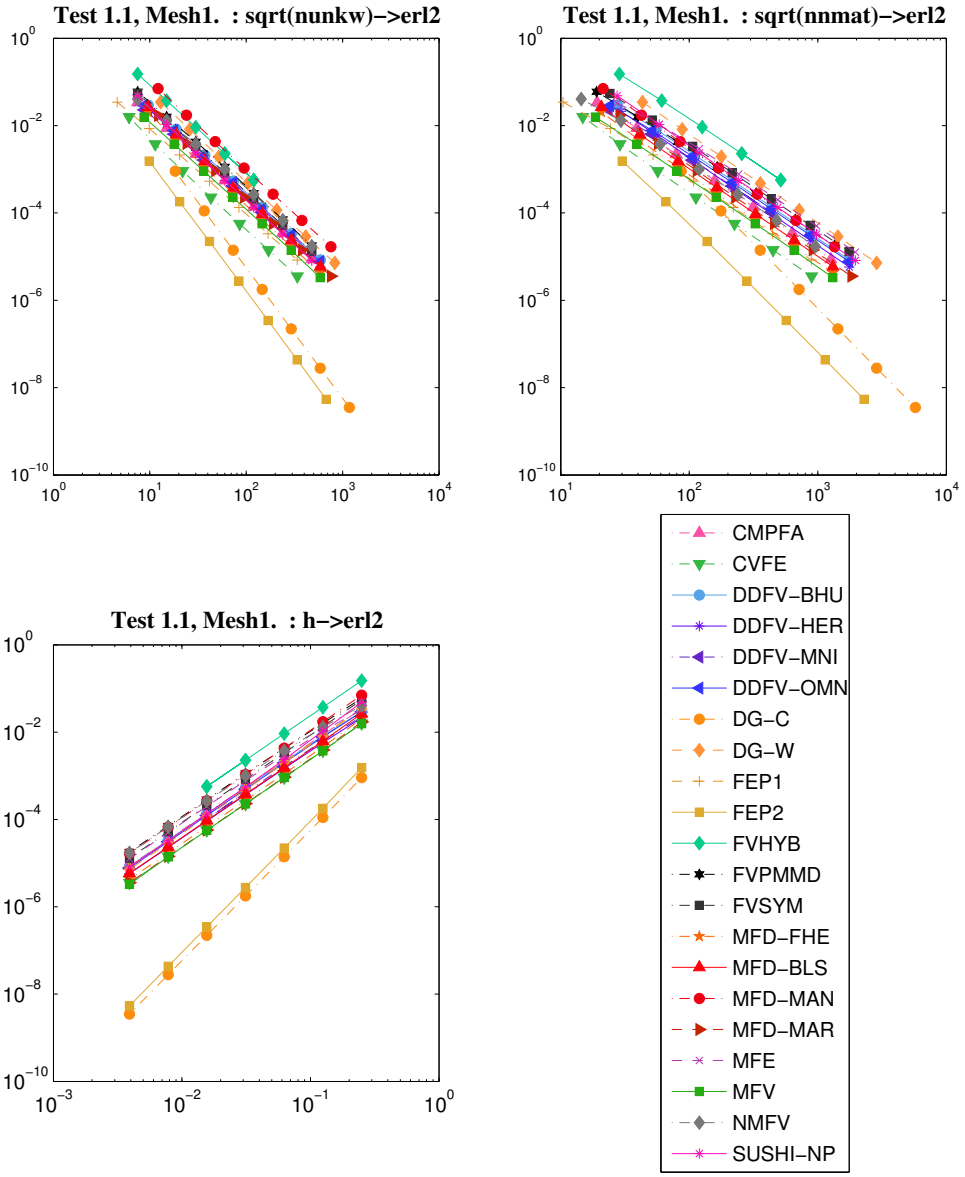

Figure 1. *L^2 norm of the solution error for test 1.1, versus* `nunknw` *(upper left),* `nnmat` *(upper right) and* `h` *(lower left) for the triangular meshes* `mesh1_i`

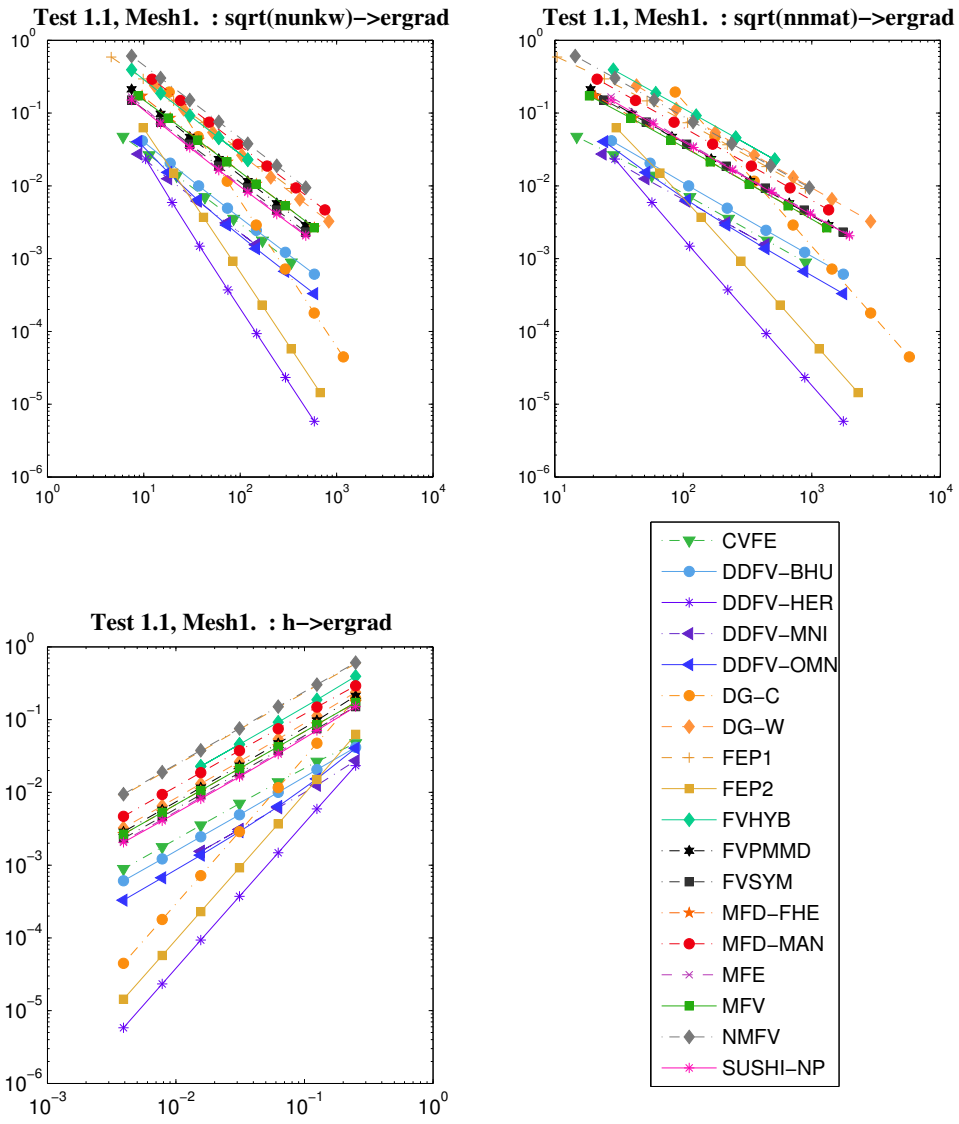

Figure 2. *L^2 norm of the gradient error for test 1.1, versus* `nunknw` *(upper left),* `nnmat` *(upper right) and* `h` *(lower left) for the triangular* `mesh1_i`

	mesh 4_1		mesh 4_2	
	umin	umax	umin	umax
CMPFA	9.95E-03	1.00E+00	2.73E-03	9.99E-01
CVFE	0.00E+00	8.43E-01	0.00E+00	9.14E-01
DDFV-BHU	1.33E-02	9.96E-01	3.63E-03	9.99E-01
DDFV-HER	0.00E+00	1.03E+00	0.00E+00	1.01E+00
DDFV-MNI	-3.09E-01	1.03E+00	0.00E+00	1.00E+00
DDFV-OMN	1.34E-02	1.03E+00	3.65E-03	1.01E+00
DG-C	-2.33E-03	9.96E-01	-3.24E-04	9.99E-01
DG-W	-7.90E-05	9.22E-01	-8.18E-06	9.66E-01
FEQ1	0.00E+00	8.61E-01	0.00E+00	9.37E-01
FEQ2	0.00E+00	9.99E-01	0.00E+00	1.00E+00
FVHYB	2.14E-03	9.84E-01	7.16E-04	9.93E-01
FVSYM	7.34E-03	9.59E-01	2.33E-03	9.89E-01
MFD-BLS	8.54E-03	9.55E-01	2.44E-03	9.87E-01
MFD-FHE	9.73E-03	9.45E-01	2.90E-03	9.83E-01
MFD-MAN	6.64E-03	9.71E-01	1.50E-03	9.93E-01
MFD-MAR	8.82E-03	9.60E-01	2.47E-03	9.88E-01
MFV	1.08E-02	9.42E-01	3.34E-03	9.82E-01
NMFV	1.30E-02	1.11E+00	3.61E-03	1.04E+00
SUSHI-NP	7.64E-03	8.88E-01	2.33E-03	9.61E-01

Table 1. *Test 1.1: Minimum and maximum of the approximate solutions for* `mesh 4_1` *and* `mesh 4_2`

The exact solution is taken to be $u(x,y) = \sin(2\pi x)e^{-2\pi\sqrt{1/\delta}y}$; note that since δ is large, the solution is almost constant in the y variable. We consider Problem [1] with non-homogeneous Neumann boundary conditions ($\Gamma_D = \emptyset$ and $\Gamma_N = \partial\Omega$), so that the right hand side is $f = -\nabla\cdot(\mathbf{K}\nabla u)$ and the Neumann boundary condition $g = (\mathbf{K}\nabla u\cdot\mathbf{n})|_{\partial\Omega}$. Furthermore, we shall ensure the uniqueness of the solution to [1] by enforcing the condition $\int_\Omega u\,dx = 0$. The meshes are the triangular meshes `mesh1`.

This test was mentioned in [**?**] as causing some numerical locking problems for finite volume and finite element schemes, and in fact, some schemes could not give the solution. We give in Tables 2 and 3 the minimum and maximum values obtained with those schemes which passed the test, and on what grid they are obtained, along with the convergence order for the error of the solution and its gradient. The behaviour of the $P1$ finite element scheme seems good except on the very first grid where, even though the maximum principle is satisfied, the maximum and minimum values are close to 0, and quite far from the exact ones; this is also the case for the schemes DG-W SUSHI-NP (but this latter scheme does not converge well on finer grids). The $P2$ finite elements also give good results, even if the rate of convergence is a bit under the theoretical rate on the last grids. Note that the scheme DDFV-OMN satisfies the discrete maximum principle for both $\delta = 10^5$ and $\delta = 10^6$. Most schemes seem to encounter

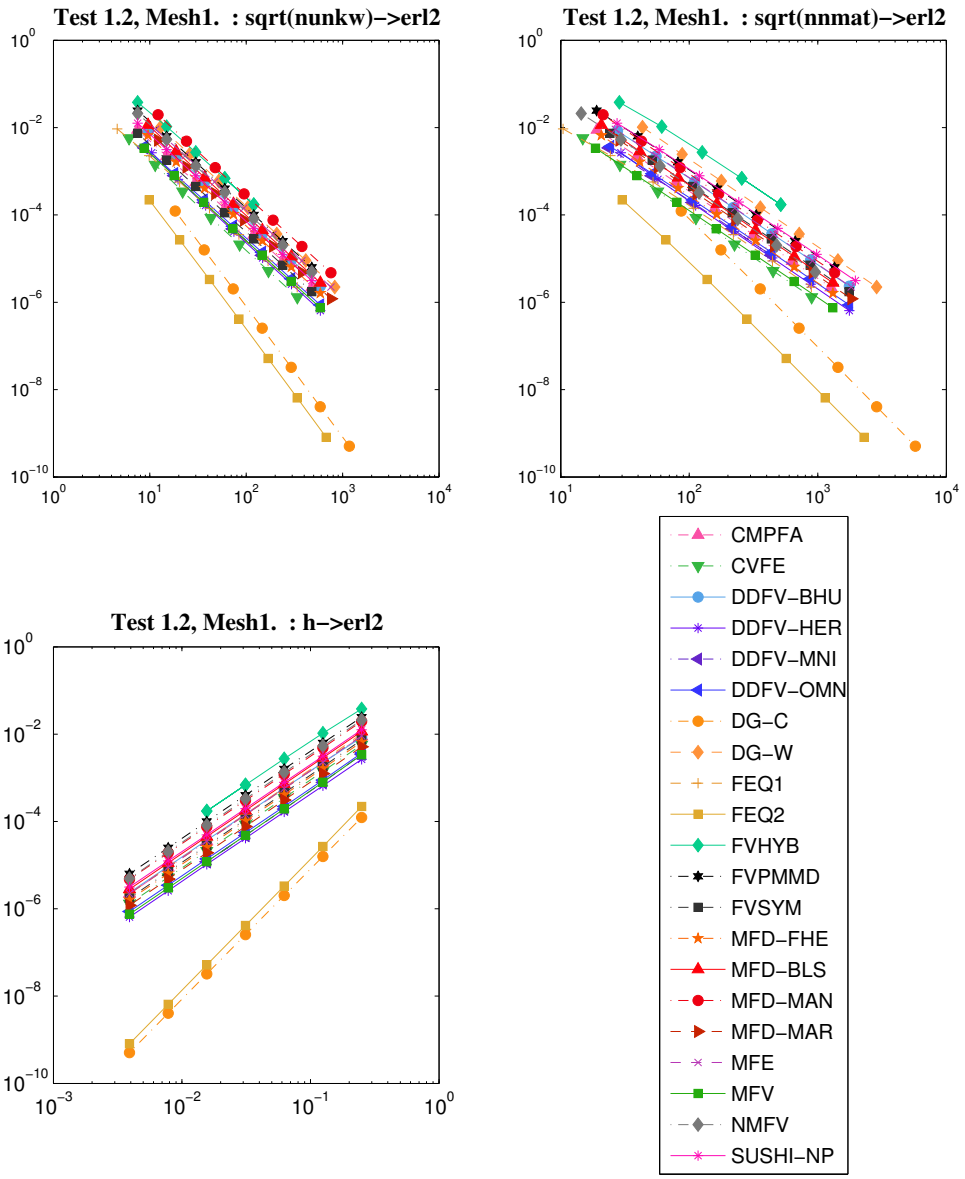

Figure 3. *L^2 norm of the solution error for test 1.2, versus* `nunknw` *(upper left),* `nnmat` *(upper right) and* `h` *(lower left) for the triangular* `mesh1_i`

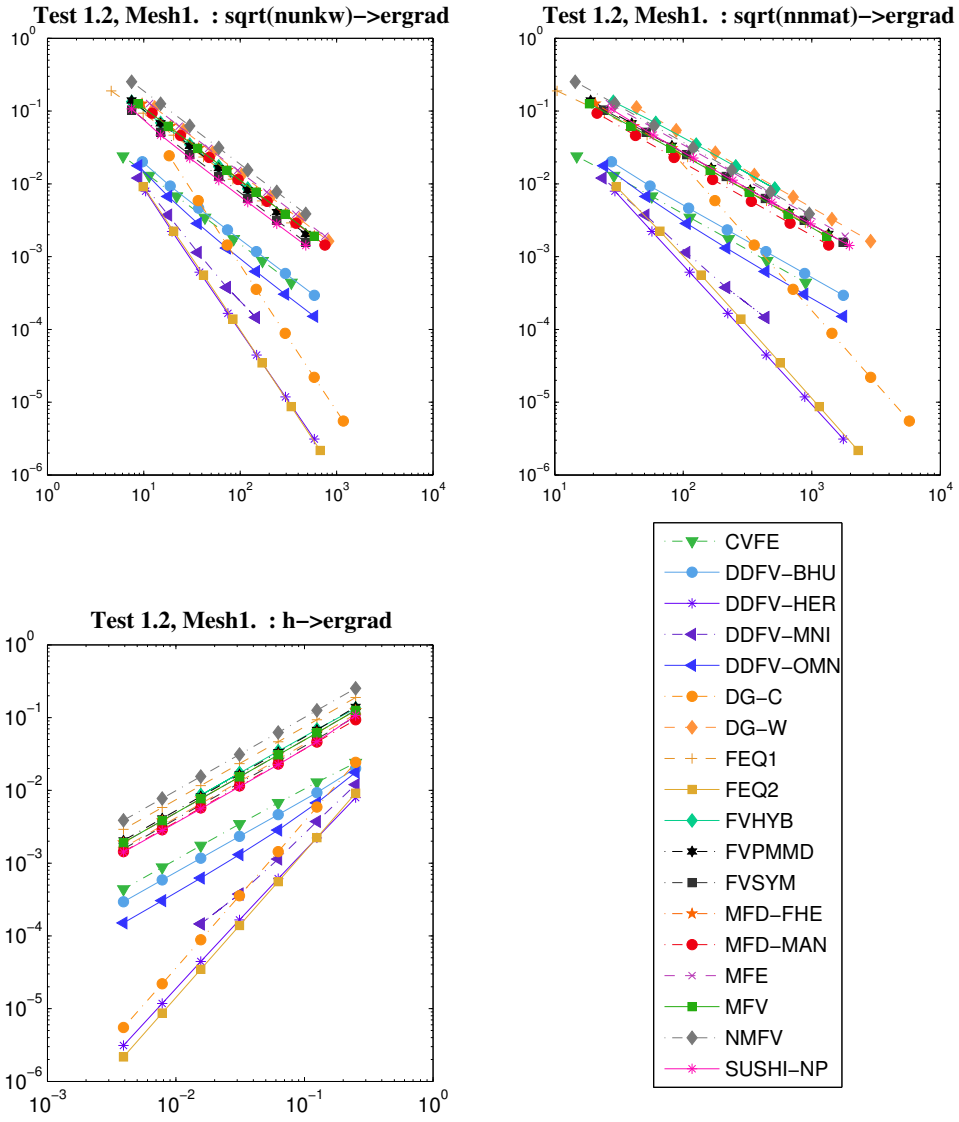

Figure 4. *L^2 norm of the gradient error for test 1.2, versus* `nunknw` *(upper left),* `nnmat` *(upper right) and* `h` *(lower left) for the triangular* `mesh1_i`

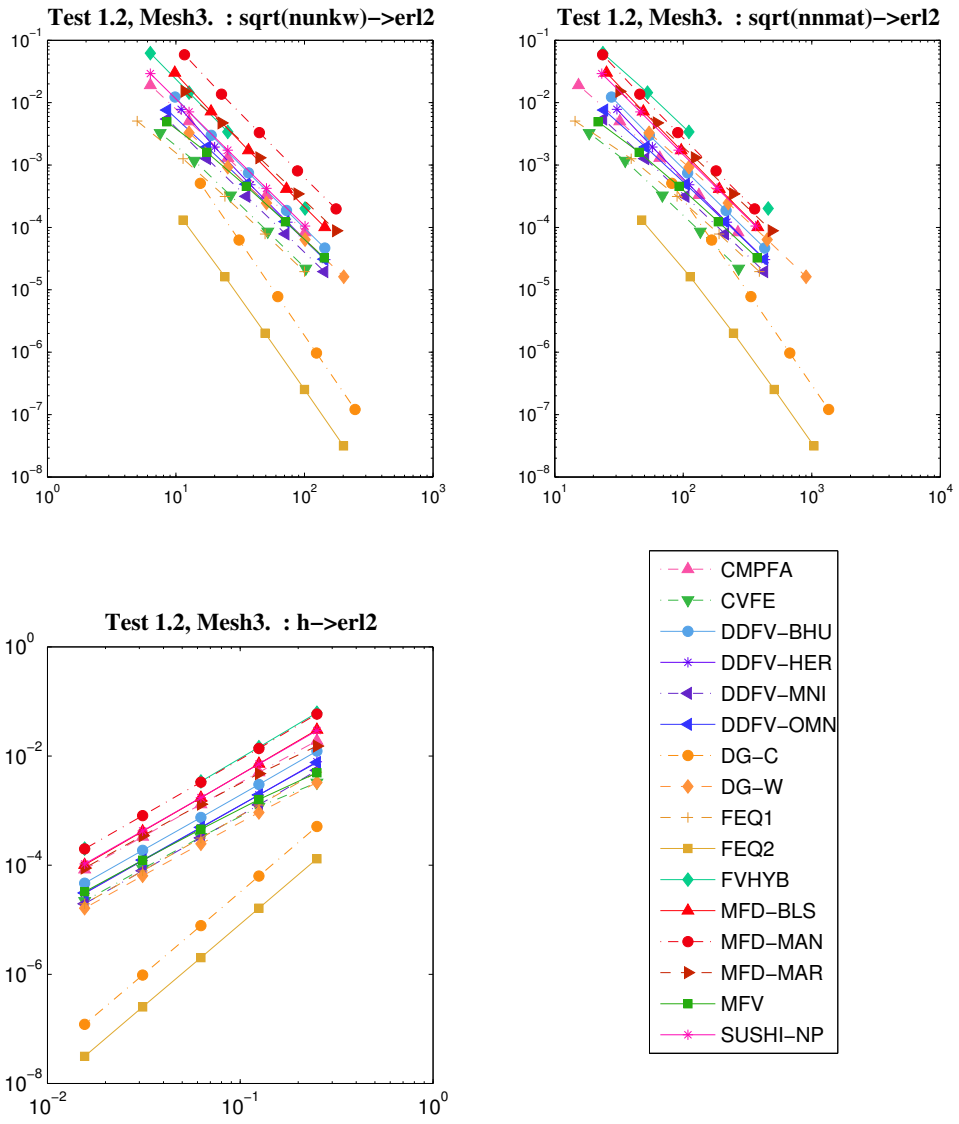

Figure 5. *L^2 norm of the solution error for test 1.2, versus* `nunknw` *(upper left),* `nnmat` *(upper right) and* `h` *(lower left), for the refined non-conforming rectangular* `mesh3_i`

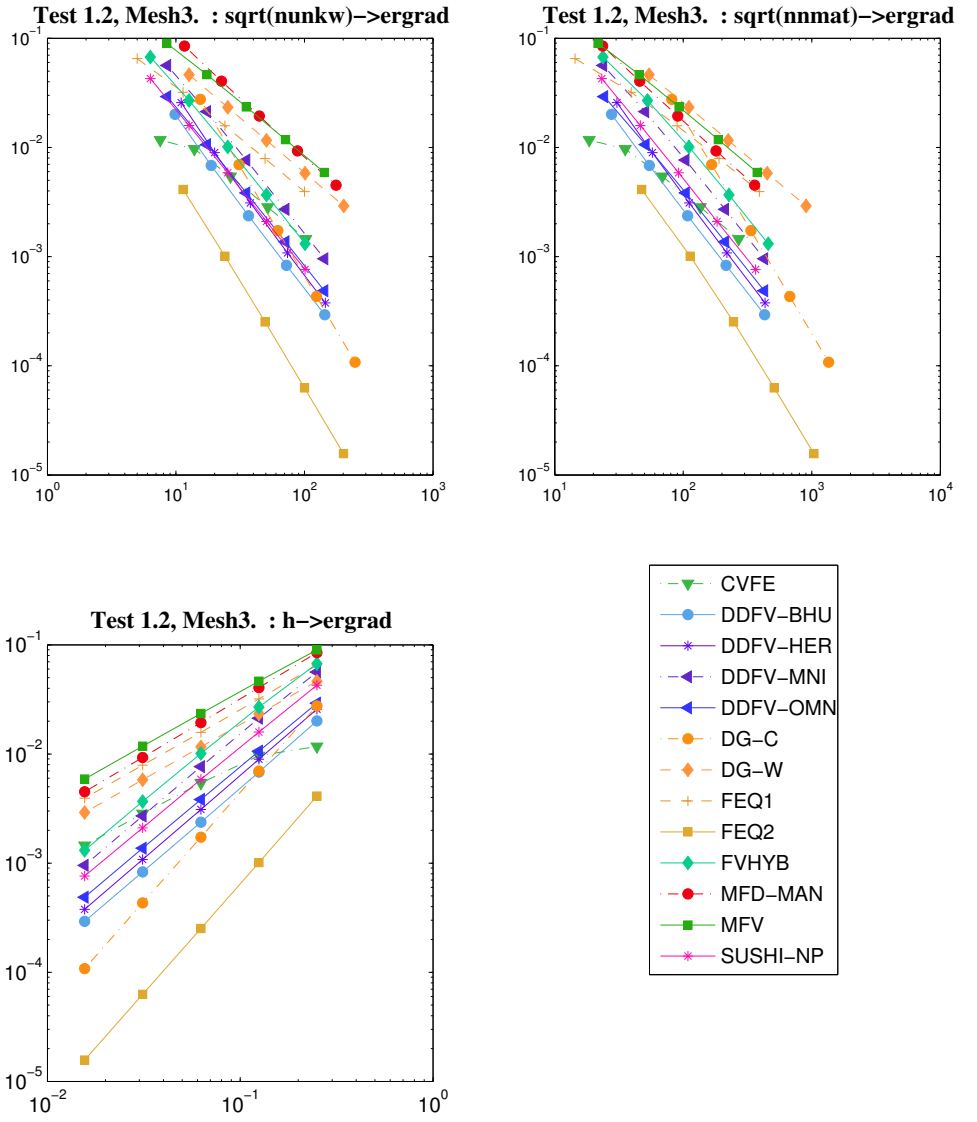

Figure 6. *L^2 norm of the gradient error for test 1.2, versus* `nunknw` *(upper left),* `nnmat` *(upper right), and* `h` *(lower left), for the refined non-conforming rectangular* `mesh3_i`

	min(umin), i	max(umax), i	ocvl2	ocvgrad	erflm
CMPFA	-1.10E+00, 1	1.04E+00, 3	1.09	/	6.36E+02
CVFE	-1.01E-00, 2	1.01E-01, 2	2.00	1.00	1.55E+01
DDFV-BHU	-9.27E-01, 1	1.17E+00, 1	1.76	1.21	7.51E+00
DDFV-HER	-4.20E-01, 2	9.12E+00, 4	/	/	7.16E-03
DDFV-OMN	-8.24E-01, 1	7.76E-01, 1	2.00	1.00	2.11E+00
DG-W	-1.18E-01, 1	1.18E-01, 1	2.00	1.00	1.69E+01
FEP1	-9.48E-03, 1	9.75E-03, 1	2.00	1.01	/
FEP2	-9.56E-01, 1	9.56E-01, 1	2.97	2.00	/
FVSYM	-1.76E+00, 2	1.80E+00, 2	2.38	1.47	7.29E+00
MFD-BLS	-6.50E+00, 2	5.75E+00, 2	2.54	/	3.59E+01
MFD-FHE	-6.50E+00, 2	5.75E+00, 2	2.54	1.51	3.59E+01
MFD-MAN	-6.62E+00, 2	5.50E+00, 2	2.49	1.50	3.58E+01
MFD-MAR	-6.50E+00, 2	5.75E+00, 2	2.53	/	3.59E+01
MFE	-6.50E+00, 2	5.75E+00, 2	2.53	1.47	3.59E+01
MFV	-6.50E+00, 2	5.75E+00, 2	2.41	1.51	3.58E+01
SUSHI-P	-6.50E+00, 2	5.75E+00, 2	2.53	1.47	3.59E+01
SUSHI-NP	-1.93E-02, 4	1.89E-02, 4	0.37	1.99	/

Table 2. *Test 2, (numerical locking)* $\delta = 10^5$

some difficulties on the first two (for $\delta = 10^5$) or three (for $\delta = 10^6$) coarsest meshes (locking effect). Note also the very similar behaviour of the schemes MFE, MFD-FHE, MFD-BLS, MFD-MAN, MFD-MAR and SUSHI-P on this test case.

6. Test 3: oblique flow

This test case represents a flow with boundary conditions such that the pressure driven flow "would like" to go from vertex (0,0) to vertex (1,1), but is impeded by a homogeneous anisotropic tensor with high permeability in a direction at 40 degrees from the horizontal and low permeability in the orthogonal direction. This test case is inspired by a talk given by I. Aavatsmark in Paris in December 2006 at GDR MOMAS. The permeability tensor is:

$$\mathbf{K} = R_\theta \begin{pmatrix} 1 & 0 \\ 0 & \delta \end{pmatrix} R_\theta^{-1},$$

where R_θ is the rotation of angle $\theta = 40$ degrees and $\delta = 10^{-3}$.

	min(umin), i	max(umax), i	ocvl2	ocvgrad	erflm
CMPFA	-1.72E+00, 1	1.72E+00, 1	2.27	/	9.84E+04
CVFE	-1.01E-00, 2	1.01E-00, 2	2.00	1.0	4.90E+01
DDFV-BHU	-9.17E-01, 1	1.19E+00, 1	2.11	1.35	1.38E+01
DDFV-HER	-2.10E-01, 2	7.10E-01, 1	/	/	1.64E-01
DDFV-OMN	-8.19E-01, 1	7.82E-01, 1	2.00	1.00	1.62
DG-W	-1.17E-01, 1	1.17E-01, 1	2.00	1.00	5.34E+01
FEP1	-2.93E-03, 1	3.02E-03, 1	2.00	0.99	/
FEP2	-9.50E-01, 1	9.50E-01, 1	2.96	2.00	/
FVSYM	-3.62E+00, 2	3.62E+00, 2	2.31	1.50	2.30E+01
MFD-BLS	-6.59E+00, 3	6.08E+00, 3	2.53	/	1.14E+02
MFD-FHE	-6.59E+00, 3	6.08E+00, 3	2.53	1.51	1.14E+02
MFD-MAN	-6.62E+00, 3	5.83E+00, 3	2.51	1.50	1.14E+02
MFD-MAR	-6.59E+00, 3	6.08E+00, 3	2.53	/	1.14E+02
MFE	-1.86E+01, 2	1.63E+01, 2	2.5	1.23	1.14E+02
MFV	-6.59E+00, 3	6.08E+00, 3	2.41	1.51	1.14E+02
SUSHI-P	-1.86E+01, 2	1.63E+01, 2	2.5	1.23	1.14E+02
SUSHI-NP	-6.48E-03, 5	6.42E-03, 5	0.046	1.98	/

Table 3. *Test 2 (numerical locking)* $\delta = 10^6$

The source term is equal to zero ($f = 0$). We use a uniform rectangular family of meshes `mesh2_i`. Dirichlet boundary conditions are considered, $\Gamma_D = \partial\Omega$ with $\bar{u}$ a continuous and piecewise linear function defined by:

$$\bar{u}(x,y) = \begin{cases} 1 & \text{on} \quad ((0,.2)\times\{0.\}\cup\{0.\}\times(0,.2) \\ 0 & \text{on} \quad ((.8,1.)\times\{1.\}\cup\{1.\}\times(.8,1.) \\ \frac{1}{2} & \text{on} \quad ((.3,1.)\times\{0\}\cup\{0\}\times(.3,1.) \\ \frac{1}{2} & \text{on} \quad ((0.,.7)\times\{1.\}\cup\{1.\}\times(0.,0.7) \end{cases}$$

The solution features a Z across the $y = x$ axis; it is depicted in Figure 7 (approximate solution obtained by the scheme DDFV-BHU on a very fine grid). The maximum principle is not always easy to verify for such a solution and is violated, on coarse and fine grid, by most DDFV implementations, the DG schemes and the scheme FVHYB (see Table 4). Note also that, as previously mentioned, the FEQ2 energy, equal to $2.42E-01$, is an upper bound of the exact energy, while the MFE energy, equal to $2.41E-01$, is a lower bound of this energy. On the coarse grid, the scheme which gives the closest energy to these values is LATTB (see Table 4). However, it may be seen in Table 5 that the scheme LATTB is not so good with respect to the fluxes, for which the scheme MFD-FHE seems to be the most accurate. From this table, we can notice that most of the schemes give a reasonable approximation of the outward flux on the boundary.

Figure 7. *Approximate solution on a fine grid for Test 3, oblique flow*

7. Test 4: vertical fault

The medium considered here is a pile of anisotropic layers with a fault in the middle, which leads to a discontinuity of the layers at $x = .5$. Each geological layer is meshed with one layer of discretization cells only. The domain Ω is decomposed as $\Omega = \Omega_1 \cup \Omega_2$, with $\Omega_2 = \Omega \setminus \Omega_1$, with $\Omega_1 = \Omega_1^\ell \cup \Omega_1^r$, and

$$\Omega_1^\ell = (0.;.5] \times \left(\bigcup_{k=0}^{4} [.05 + 2k \times .1; .05 + (2k+1) \times .1) \right),$$
$$\Omega_1^r = (.5;1) \times \left(\bigcup_{k=0}^{4} [2k \times .1; (2k+1) \times .1) \right).$$

It is described in Figure 8 where Ω_1 is in black and Ω_2 in white. The diffusion tensor

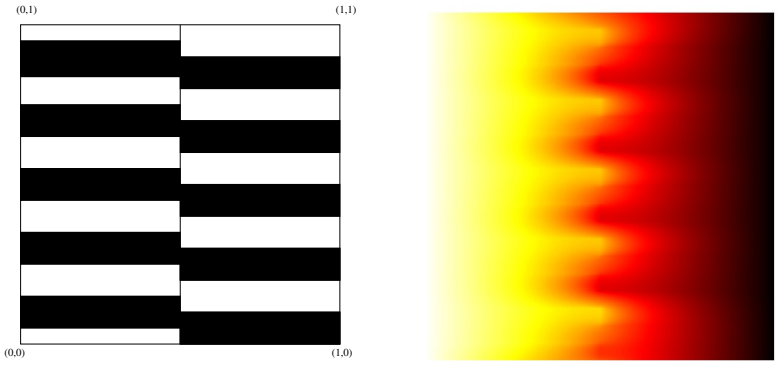

Figure 8. *The computational domain and approximate solution on a fine grid (*320×320*) for Test 4, vertical fault*

	umin_i	umax_i	ener1	eren_i	i
CMPFA	6.90E-02	9.31E-01	/	/	1
	9.83E-04	9.99E-01	/	/	7
CVFE	0.00E+00	1.00E+00	2.24E-01	8.42E-02	1
	0.00E+00	1.00E+00	2.42E-01	3.33E-03	7
DDFV-BHU	-4.72E-03	1.00E+00	2.14E-01	9.60E-02	1
	-5.31E-04	1.00E+00	2.42E-01	7.11E-06	7
DDFV-HER	-4.72E-03	1.00E+00	2.14E-01	9.46E-02	1
	-5.96E-08	1.00E+00	2.42E-01	1.91E-05	7
DDFV-MNI	-4.73E-03	1.00E+00	2.14E-01	9.61E-02	1
	-1.07E-03	1.00E+00	2.42E-01	1.86E-04	5
DDFV-OMN	1.04E-01	8.96E-01	1.81E-01	3.68E-03	1
	1.01E-03	9.99E-01	2.42E-01	1.77E-06	7
DG-C	-9.35E-02	1.07E+00	5.04E-01	9.88E-02	1
	-1.32E-03	1.00E+00	2.42E-02	2.48E-05	7
DG-W	-4.11E-02	1.04E+00	1.90E-01	5.67E-01	1
	-3.71E-03	1.00E+00	2.44E-01	2.85E-05	7
FEQ1	0.00E+00	1.00E+00	2.21E-01	3.67E-01	1
	0.00E+00	1.00E+00	2.44E-01	3.17E-02	7
FEQ2	0.00E+00	1.00E+00	2.64E-01	3.41E-01	1
	0.00E+00	1.00E+00	2.42E-01	0.00E+00	7
FVHYB	-1.75E-01	1.17E+00	2.13E-01	2.55E-01	1
	-1.00E-03	1.00E+00	2.42E-01	8.19E-03	6
FVSYM	6.85E-02	9.32E-01	2.20E-01	0.00E+00	1
	4.92E-04	9.99E-01	2.42E-01	0.00E+00	8
LATTB	1.14E-01	8.86E-01	2.42E-01	1.64E-02	1
	9.36E-04	9.99E-01	2.42E-01	3.00E-04	7
MFD-BLS	6.09E-02	9.39E-01	2.38E-01	4.44E-15	1
	1.29E-03	9.99E-01	2.42E-01	6.74E-13	7
MFD-FHE	7.06E-02	/	2.19E-01	2.09E-01	1
	1.00E-03	9.99E-01	2.42E-01	1.05E-04	7
MFD-MAN	7.56E-02	9.24E-01	1.91E-01	1.87E-14	1
	8.01E-04	9.99E-01	2.42E-01	3.70E-14	8
MFD-MAR	6.09E-02	9.39E-01	2.38E-01	9.85E-13	1
	1.00E-03	9.99E-01	2.42E-01	1.97E-10	8
MFE	3.12E-02	9.69E-01	1.25E-01	2.46E-02	1
	5.08E-04	9.99E-01	2.41E-01	2.91E-03	8
MFV	1.22E-02	8.78E-01	4.85E-01	8.23E-07	1
	7.92E-04	9.99E-01	2.42E-01	9.74E-06	7
NMFV	1.11e-01	8.88e-01	2.33e-01	1.45e-01	1
	1.28E-03	9.99E-01	2.45E-01	1.94E-02	7
SUSHI-NP	6.03E-02	9.40E-01	2.25E-01	3.01E-01	1
	8.52E-04	9.99E-01	2.43E-01	1.28E-02	7

Table 4. *Test 3, the values of umin, umax and the energies*

	flux0_i	flux1_i	fluy0_i	fluy1_i	i
CMPFA	-1.94E-01	1.94E-01	-1.18E-01	1.18E-01	1
	-1.93E-01	1.93E-01	-9.87E-02	9.87E-02	7
CVFE	-2.28E-01	2.28E-01	-1.86E-01	1.86E-01	1
	-1.94E-01	1.94E-01	-9.97E-02	9.97E-02	7
DDFV-BHU	-1.82E-01	1.82E-01	-1.20E-01	1.20E-01	1
	-1.93E-01	1.93E-01	-9.86E-02	9.86E-02	7
DDFV-HER	-1.82E-01	1.82E-01	-1.21E-01	1.21E-01	1
	-1.93E-01	1.93E-01	-9.85E-02	9.85E-02	7
DDFV-MNI	-1.83E-01	1.83E-01	-1.21E-01	1.21E-01	1
	-1.94E-01	1.94E-01	-9.82E-02	9.82E-02	5
DDFV-OMN	-1.80E-01	1.80E-01	-1.35E-01	1.35E-01	1
	-1.93E-01	1.93E-01	-9.86E-02	9.86E-02	7
DG-C	-1.88E-01	1.60E-01	-1.60E-01	1.88E-01	1
	-1.93E-01	1.93E-01	-9.87E-02	9.87E-02	7
DG-W	-1.71E-01	1.71E-01	-9.93E-02	9.93E-02	1
	-1.93E-01	1.93E-01	-9.86E-02	9.86E-02	7
FEQ1	-3.05E-01	3.05E-01	-2.50E-01	2.50E-02	1
	-1.94E-01	1.94E-01	-9.93E-02	9.93E-02	7
FEQ2	-1.27E-01	1.27E-01	-3.60E-02	3.60E-02	1
	-1.93E-01	1.93E-01	-9.86E-02	9.86E-02	7
FVHYB	-2.47E-01	2.47E-01	-1.86E-01	1.86E-01	1
	-1.95E-01	1.95E-01	-1.01E-01	1.01E-01	6
FVSYM	-1.95E-01	1.95E-01	-1.18E-01	1.18E-01	1
	-1.93E-01	1.93E-01	-9.87E-02	9.87E-02	8
LATTB	-1.46E-01	-2.57E-01	-1.52E-01	5.57E-01	1
	-1.96E-01	1.96E-01	-9.56E-02	9.56E-02	7
MFD-BLS	-1.97E-01	1.97E-01	-1.15E-01	1.15E-01	1
	-1.93E-01	1.93E-01	-9.87E-02	9.87E-02	7
MFD-FHE	-1.93E-01	1.93E-01	-9.57E-02	9.57E-02	1
	-1.93E-01	1.93E-01	-9.87E-02	9.87E-02	7
MFD-MAN	-2.12E-01	2.12E-01	-1.44E-01	1.44E-01	1
	-1.93E-01	1.93E-01	-9.87E-02	9.87E-02	8
MFD-MAR	-1.97E-01	1.97E-01	-1.15E-01	1.15E-01	1
	-1.93E-01	1.93E-01	-9.87E-02	9.87E-02	8
MFE	-2.67E-01	2.67E-01	- 2.22E-01	2.22E-01	1
	-1.93E-01	1.93E-01	-9.88E-02	9.88E-02	8
MFV	-8.52E-02	8.52E-02	8.52E-02	-8.52E-02	1
	-1.93E-01	1.93E-01	-9.87E-02	9.87E-02	7
NMFV	-1.71e-01	1.72e-01	-1.66e-01	1.65e-01	1
	-1.94E-01	1.94E-01	-9.79E-02	9.76E-02	7
SUSHI-NP	-1.80E-01	1.80E-01	-1.14E-01	1.14E-01	1
	-1.93E-01	1.93E-01	-9.85E-02	9.85E-02	7

Table 5. *Test 3, the fluxes*

$\mathbf{K}$ is anisotropic and heterogeneous, and is given by:

$$\mathbf{K} = \begin{pmatrix} \alpha & 0 \\ 0 & \beta \end{pmatrix}, \text{ with } \begin{cases} \begin{pmatrix} \alpha \\ \beta \end{pmatrix} = \begin{pmatrix} 10^2 \\ 10 \end{pmatrix} \text{ on } \Omega_1, \\ \begin{pmatrix} \alpha \\ \beta \end{pmatrix} = \begin{pmatrix} 10^{-2} \\ 10^{-3} \end{pmatrix} \text{ on } \Omega_2 \end{cases}$$

A Dirichlet boundary condition is imposed: $\bar{u}(x, y) = 1 - x$ on $\Gamma_D = \partial\Omega$ (so that $\Gamma_N = \emptyset$) and the right hand side is assumed equal to zero $f = 0$. Note that the exact solution of this problem should stay between 0 and 1; it is therefore interesting to see whether the schemes respect these bounds (discrete maximum principle), especially on coarse meshes (which are used in oil industry, for instance). Problem [1] is discretized using the non-conforming rectangular mesh `mesh5` (see Figure 16), the conforming 20×20 square mesh $\texttt{mesh5}_{reg}$ and a reference mesh, for instance the 320×320 square mesh $\texttt{mesh5}_{ref}$.

	umin	umax	ener1	eren
CMPFA	4.55E-02	9.56E-01	/	/
CVFE	0.00E+00	1.00E+00	45.9	1.04E-02
DDFV-BHU	4.04E-02	9.61E-01	42.1	3.65E-02
DDFV-HER	0.00E+00	1.00E+00	49.3	1.75E-01
DDFV-OMN	4.04E-02	9.62E-01	42.2	3.65E-02
DG-W	-3.34E-01	1.33E+00	43.5	1.38E-02
FVHYB	4.52E-02	9.59E-01	41.4	6.12E-02
MFD-BLS	3.31E-02	9.71E-01	33.9	7.93E-14
MFD-MAN	2.84E-02	9.75E-01	31.4	1.16E-12
MFD-MAR	4.03E-02	9.60E-01	41.1	1.30E-13
MFV	4.93E-02	9.54E-01	49.9	4.21E-05
NMFV	4.33E-02	9.58E-01	/	/
SUSHI-NP	1.32E-03	9.99E-01	39.1	6.67E-02

Table 6. *Test 4, non-conforming rectangular mesh:* `mesh5`. *The values of* `umin`, `umax` *and the energies*

From Table 8, we see that the energies given by the FEQ1 scheme and the MFE scheme on the reference mesh are both equal to 43.2, which means that this is also the value of the continuous energy. On the fine mesh, all schemes give an approximate energy which is close to this value, and the results on the fluxes are also quite homogeneous. If we now look at what are the schemes that give the energy which is closest to 43.2 on the coarse mesh (Table 6), we find that the closest is given by DG-W (error of less than 0.5 %), and that the outward fluxes (Table 7) given by DG-W are also close to the reference ones (Table 9). However, neither the upper nor the lower bound is respected by the scheme. This illustrates the well-known fact that precision and robustness are difficult to obtain simultaneously. Other schemes (DDFV-BHU, DDFV-OMN, FVHYB, MFD-MAR, SUSHI-NP) give an energy and fluxes which are reasonably close to the reference ones (some schemes are better for the energy, other better for

	flux0	flux1	fluy0	fluy1
CMPFA	-45.2	46.1	-0.95	4.84E-04
CVFE	-46.6	48.5	0.87	8.02E-04
DDFV-BHU	-40.0	41.8	-1.81	9.08E-04
DDFV-HER	-40.0	41.8	-1.81	9.08E-04
DDFV-MNI	-43.8	45.5	-2.8	1.18E+00
DDFV-OMN	-40.0	41.8	-1.81	9.08E-04
DG-W	-43.1	45.3	-2.19	1.50E-03
FVHYB	-44.3	46.3	0.49	1.55E-04
MFD-BLS	-32.3	36.2	-3.94	1.22E-03
MFD-MAN	-29.7	34.1	-4.37	1.01E-03
MFD-MAR	-39.8	42.5	-2.68	9.95E-04
MFV	-44.0	50.3	-8.03	1.72E+00
NMFV	-43.2	44.5	-1.23	2.32E-04
SUSHI-NP	-40.9	43.1	-2.21	6.94E-04

Table 7. *Test 4, non-conforming rectangular mesh:* `mesh5`. *The fluxes*

	umin	umax	ener1	eren
CMPFA	1.32E-03	9.99E-01	/	/
CVFE	0.00E+00	1.00E+00	43.3	6.25E-04
DDFV-BHU	1.31E-03	9.98E-01	43.2	1.27E-03
DDFV-HER	0.00E+00	1.00E+00	43.8	1.64E-02
DDFV-MNI	00E+00	1.00E+00	43.8	6.23E-02
DDFV-OMN	1.32E-03	9.99E-01	43.2	1.28E-03
DG-C	-2.20E-06	1.00E+00	43.2	1.46E-04
DG-W	-2.21E-09	1.00E+00	43.2	7.63E-04
FEQ1	0.00E+00	1.00E+00	43.3	2.31E-03
FEQ2	0.00E+00	1.00E+00	43.2	0.00E+00
MFD-BLS	1.32E-03	9.99E-01	43.2	2.84E-12
MFD-FHE	2.12E-02	1.00E+00	43.2	3.53E-04
MFD-MAN	1.32E-03	9.99E-01	43.2	4.71E-14
MFD-MAR	1.32E-03	9.99E-01	43.2	2.69E-12
MFE	1.32E-03	9.99E-01	43.2	4.20E-04
MFV	1.32E-03	9.99E-01	43.2	1.88E-05
NMFV	1.32E-03	9.99E-01	43.2	5.92E-04
SUSHI-NP	1.32E-03	9.99E-01	43.1	8.88E-04

Table 8. *Test 4, the square* 320×320 *mesh* $\texttt{mesh5}_{ref}$. *The values of* `umin`, `umax` *and the energies*

the fluxes), while respecting the discrete maximum principle. Note that the MFD implementations MFD-BLS and MFD-MAN give surprisingly low values of both energy and fluxes in comparison with MFD-MAR.

	flux0	flux1	fluy0	fluy1
CMPFA	-42.1	44.4	-2.33	7.97E-04
CVFE	-42.2	44.5	-2.25	7.98E-04
DDFV-BHU	-42.1	44.4	-2.33	7.94E-04
DDFV-HER	-42.0	44.3	-2.35	7.97E-04
DDFV-MNI	-39.9	42.6	-2.68	8.01E-04
DDFV-OMN	-42.1	44.4	-2.33	7.97E-04
DG-C	-42.1	44.5	-2.32	7.98E-04
DG-W	-42.1	44.5	-2.32	7.96E-04
FEQ1	-42.2	44.5	-2.16	7.96E-04
FEQ2	-42.1	44.5	-2.32	7.96E-04
MFD-BLS	-42.1	44.4	-2.33	7.96E-04
MFD-FHE	-42.1	44.5	-2.47	7.98E-04
MFD-MAN	-42.1	44.4	-2.33	7.97E-04
MFD-MAR	-42.1	44.4	-2.33	7.96E-04
MFE	-42.1	44.4	-2.33	-7.96E-04
MFV	-42.1	44.4	-2.33	8.33E-04
NMFV	-42.1	44.4	-2.33	7.97E-04
SUSHI-NP	-42.1	44.4	-2.33	7.97E-04

Table 9. *Test 4, the square* 320×320 *mesh* $\texttt{mesh5}_{ref}$. *The fluxes*

8. Test 5: heterogeneous rotating anisotropy

This test is inspired from [**?**, **?**]. The permeability tensor is a rotating anisotropic tensor:

$$\mathbf{K} = \frac{1}{(x^2+y^2)} \begin{pmatrix} 10^{-3}x^2 + y^2 & (10^{-3}-1)xy \\ (10^{-3}-1)xy & x^2 + 10^{-3}y^2 \end{pmatrix},$$

and we consider the following smooth exact solution:

$$u(x,y) = \sin \pi x \sin \pi y,\ f = -\nabla \cdot (\mathbf{K} \nabla u).$$

Problem [1] is then solved with non-homogeneous boundary conditions: $\Gamma_D = \partial\Omega$, $\Gamma_N = \emptyset$ and $\bar{u}(x,y) = \sin \pi x \sin \pi y$, and approximated on the uniform rectangular `mesh2`.

We give in Figure 9 the L^2 norm of the error versus the number of unknowns (upper left), the square root of the number of non-zero matrix terms (upper right) and the step size `h` (lower left) for all schemes for meshes `mesh2`. As can be seen in Figure 9, all schemes show an order 2 convergence except for the two higher order schemes FEP2 and DG-C, which are order 3. As for the L^2 norm of the gradient is concerned, all the schemes, even higher order schemes, show an order 2 convergence, with an error with respect to `nunkw`, `nnmat` and `h` minimized by the DDFV schemes (see Figure 10).

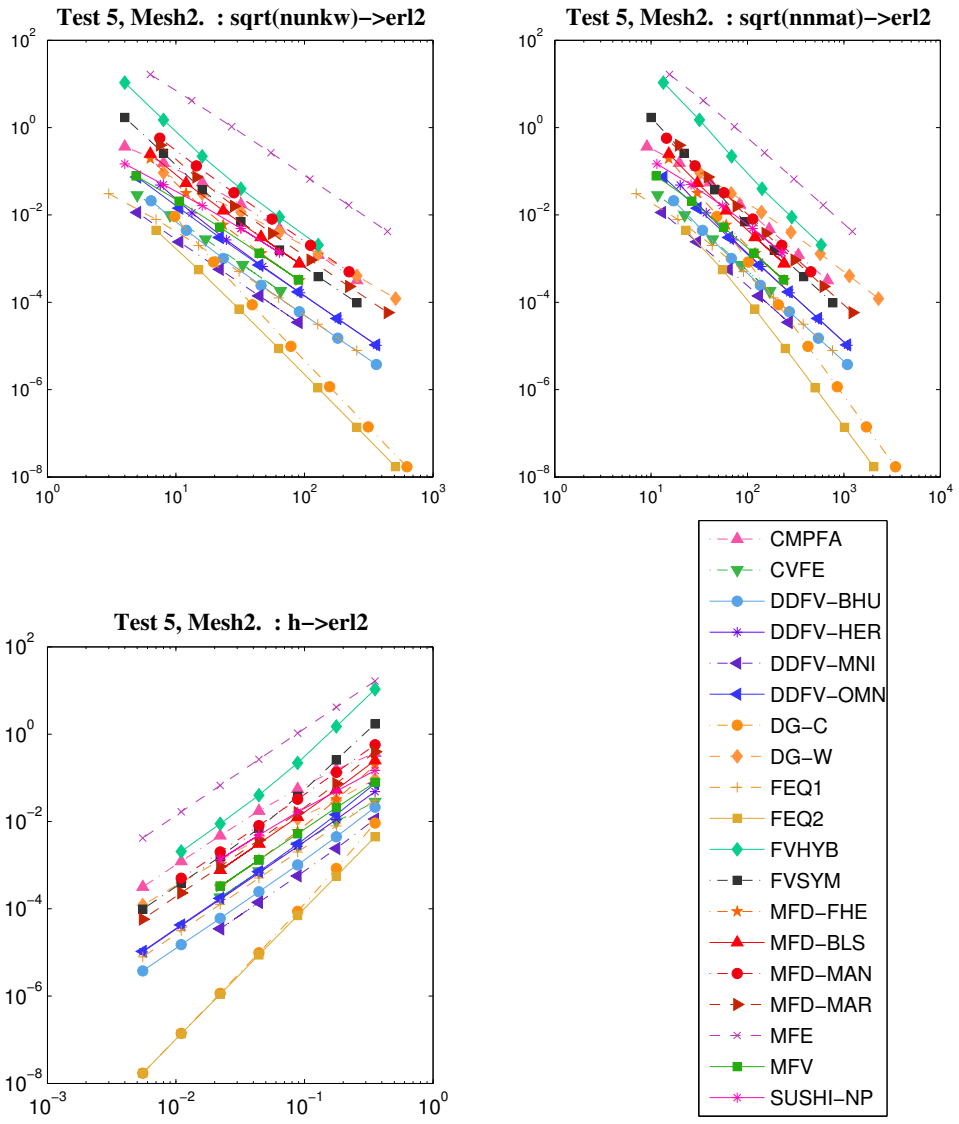

Figure 9. *L^2 norm of the solution error for test 5, versus* `nunknw` *(upper left),* `nnmat` *(upper right) and* `h` *(lower left), for the rectangular mesh* `mesh2`

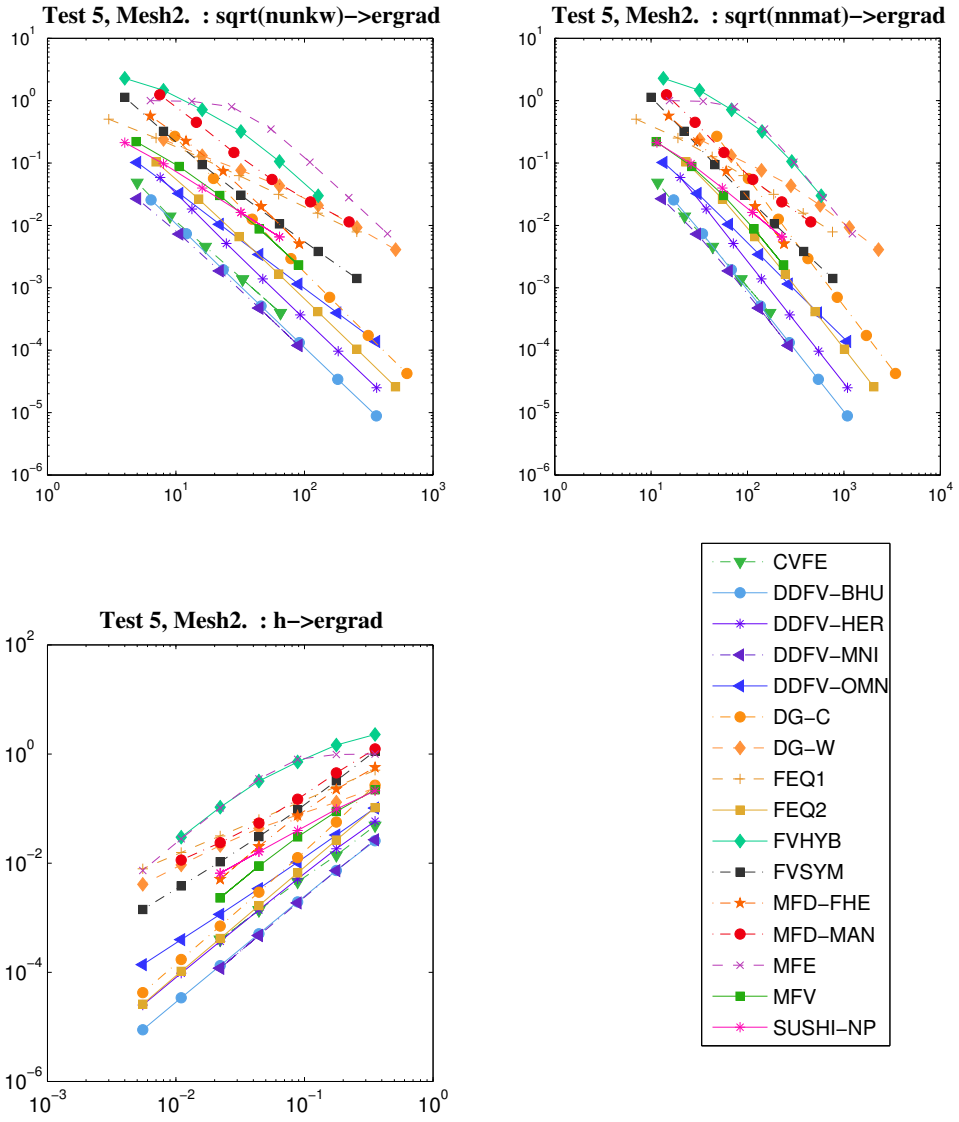

Figure 10. *L^2 norm of the gradient error for test 5, versus* `nunknw` *(upper left),* `nnmat` *(upper right) and* `h` *(lower left), for the rectangular mesh* `mesh2`

	umin	umax
CMPFA	-1.06E-01	1.09E+00
DDFV-HER	0.00E+00	1.01E+00
DG-C	-7.95E-04	1.02E+00
DG-W	-7.68E-02	1.06E+00
FEQ1	0.00E+00	1.05E+00
FVHYB	-1.92E+01	5.38E+00
FVSYM	-8.67E-01	2.57E+00
MFE	-1.62E+00	1.90E+01

Table 10. *Test 5: minimum and maximum values on the coarsest mesh for the schemes which do not satisfy the maximum principle*

All schemes converge when the mesh is refined, but some schemes violate the discrete maximum principle, as may be seen in Table 10. Note that the schemes MFE and FVHYB violate it even on the fine grids.

9. Test 6: oblique drain

This test case represents a situation which is encountered in underground flow engineering where an oblique drain consisting in a very permeable layer concentrates most part of the flow; this drain is meshed with only one layer of discretization cells. In the case of a pressure gradient driven transport, as often described in reservoir engineering, it seems important that the discretization cells consist in only one homogeneous material: numerical experiments show that otherwise the solution may be badly approximated. Here we consider the steady case, but wish to verify that the outward fluxes are as close as possible to the exact values for the meshes considered here, both for the conforming and non-conforming meshes.

The domain Ω is composed of 3 subdomains:

$$\begin{aligned}\Omega_1 &= \{(x,y)\in\Omega; \phi_1(x,y)<0\},\\ \Omega_2 &= \{(x,y)\in\Omega; \phi_1(x,y)>0, \phi_2(x,y)<0\},\\ \Omega_3 &= \{(x,y)\in\Omega; \phi_2(x,y)>0\},\end{aligned}$$

with $\phi_1(x,y) = y - \delta(x-.5) - .475$ and $\phi_2(x,y) = \phi_1(x,y) - 0.05$.

We take the slope of the drain $\delta = 0.2$ and define the exact solution and the source term by:

$$u(x,y) = -x - \delta y, \text{ on } \Omega,\ f = -\nabla(\mathbf{K}\nabla u),$$

where the permeability tensor $\mathbf{K}$ is such that its principal axes are parallel and perpendicular to the drain:

$$\mathbf{K} = R_\theta \begin{pmatrix} \alpha & 0 \\ 0 & \beta \end{pmatrix} R_\theta^{-1},$$

with θ such that $\delta = \tan\theta$ and:

$$\begin{pmatrix} \alpha \\ \beta \end{pmatrix} = \begin{pmatrix} 10^2 \\ 10 \end{pmatrix} \text{ on } \Omega_2 \quad \text{and} \quad \begin{pmatrix} \alpha \\ \beta \end{pmatrix} = \begin{pmatrix} 1 \\ 10^{-1} \end{pmatrix}, \text{ on } \Omega_1 \cup \Omega_3.$$

Problem [1] is considered with non-homogeneous Dirichlet boundary conditions: $\Gamma_D = \partial\Omega$, $\Gamma_N = \emptyset$ and $\bar{u}(x,y) = -x - \delta y$, and approximated on the conforming mesh: `mesh6` and the non-conforming mesh `mesh7`.

As the exact solution is affine on the whole domain, only a few schemes (CVFE, DDFV-HER, MFV, NMFV) are not exact on such a problem. Moreover, they all satisfy the discrete maximum principle. The interest of this case lies in the approximation of the interface fluxes, which could be used for instance for the approximation of a coupled system of diffusion and convection equations.

10. Test 7: oblique barrier

This test case is similar to the Test 6, except that we now have to deal with a barrier, and the aim is that the scheme should respect this barrier as well as the outward fluxes.

We take the same geometry as test 6 above, with the slope of the drain $\delta = 0.2$.

We take the exact solution to be

$$u(x,y) = \begin{cases} -\phi_1(x,y) \text{ on } \Omega_1, \\ -\phi_1(x,y)/10^{-2} \text{ on } \Omega_2, \\ -\phi_2(x,y) - 0.05/10^{-2} \text{ on } \Omega_3, \end{cases}$$

and $f = -\nabla\cdot(\mathbf{K}\nabla u)$, where the permeability tensor K is heterogeneous and isotropic:

$$\mathbf{K} = \begin{pmatrix} \alpha & 0 \\ 0 & \alpha \end{pmatrix}, \text{ with } \alpha = \begin{cases} 1 & \text{on } \Omega_1 \cup \Omega_3, \\ 10^{-2} & \text{on } \Omega_2. \end{cases}$$

We consider Problem [1] with Dirichlet boundary conditions: $\Gamma_D = \partial\Omega$, $\Gamma_N = \emptyset$, and $\bar{u} = u|_{\partial\Omega}$, and discretize the problem using the mesh `mesh6`.

The exact solution of this problem being piecewise affine, most of the schemes are exact on this test; the non-exact schemes are: CVFE, DDFV-HER, DDFV-OMN, MFV, NMFV. A few schemes (namely some DDFV and DG schemes) have values which are less than the exact minimum (see Table 11).

11. Test 8: perturbed parallelograms [?]

This test case was given to us by I. Aavatsmark [**?**], and is meant to test the schemes for the violation of the maximum principle within the domain. The domain Ω is a parallelogram, which is represented in Figure 11. The parameters shown in Figure 11 are $X = 1$, $Y = 1/30$ and $\theta = 30°$.

	erl2	ergrad	umin	umax
CMPFA	1.23E-15	/	-5.54	5.37E-01
CVFE	1.83E-05	3.86E-05	-5.57	5.75E-01
DDFV-BHU	1.38E-14	5.86E-14	-5.575	5.75E-01
DDFV-HER	6.53E-08	/	-5.575	5.75E-01
DDFV-MNI	1.38E-15	3.48E-14	-5.58	5.75E-01
DDFV-OMN	3.79E-08	4.51E-08	-5.58	5.75E-01
DG-C	1.39E-13	1.88E-12	-5.58	5.75E-01
DG-W	1.18E-14	1.89E-14	-5.58	5.75E-01
FEQ1	3.79E-15	6.49E-14	-5.575	5.75E-01
FEQ2	6.12E-15	8.19E-14	-5.575	5.75E-01
FVHYB	1.24E-15	5.10E-14	-5.54	5.37E-01
FVSYM	ϵ	ϵ	-5.53	5.37E-01
MFD-BLS	ϵ	/	-5.54	5.37E-01
MFD-FHE	3.25E-15	4.73E-15	-5.54	5.37E-01
MFD-MAN	1.39E-15	1.92E-15	-5.54	5.37E-01
MFD-MAR	8.19E-13	/	-5.54	5.37E-01
MFV	1.40E-08	4.69E-08	-5.54	5.37E-01
NMFV	4.98E-03	/	-5.54	5.37E-01
SUSHI-NP	1.30E-15	1.35E-14	-5.54	5.37E-01

Table 11. *Test 7, the conforming mesh:* `mesh6` *(ϵ = machine precision)*

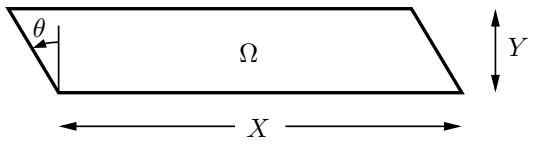

Figure 11. *Parallelogram-shaped domain Ω showing the distances X and Y and the angle θ*

The medium is homogeneous and isotropic with $\mathbf{K} = Id$. Problem [1] is considered with homogeneous Dirichlet boundary conditions: $\Gamma_D = \partial\Omega$, $\Gamma_N = \emptyset$ on the perturbed parallelogram mesh `mesh8`; see Figure 18.

The source term f is equal to zero ($f = 0$) in all cells except cell $(6, 6)$ where

$$\int_{\text{cell}(6,6)} f(x)\, dx = 1.$$

Note that the solution u of this problem should be a function with a maximum in cell $(6, 6)$, decreasing smoothly to zero towards the boundary. If u shows internal oscillations or if $u < 0$, Hopf's first lemma is violated.

	umin	umax		umin	umax
Fine grid	1.07E-24	4.10E-01			
CMPFA	-2.31E-02	1.03E-01	FVHYB	-3.38E-02	1.12E-01
CVFE	-1.23E-03	4.24E-02	FVSYM	-7.21E-02	1.52E-01
DDFV-BHU	-1.25E-03	8.22E-02	FVPMMD	1.22E-09	3.99E-01
DDFV-HER	-1.61E-03	8.99E-02	MFD-BLS	-1.03E-01	1.85E-01
DDFV-MNI	-1.46E-03	6.69E-02	MFD-FHE	-6.54E-02	1.44E-01
DDFV-OMN	-1.77E-03	8.36E-02	MFD-MAR	-2.62E-02	9.07E-02
DG-C	-7.33E-03	1.05E-01	MFV	-8.08E-03	5.81E-02
DG-W	-9.03E-03	6.57E-02	NMFV	3.05E-15	9.42E-02
FEQ1	-4.17E-03	4.90E-02	SUSHI-NP	-1.19E-03	5.65E-02
FEQ2	-5.07E-03	8.04E-02	SUSHI-P	3.26E-06	6.77E-03

Table 12. *Minimum and maximum values for Test 8*

	flux0	flux1	fluy0	fluy1
Fine grid	5.46E-21	5.46E-21	5.00E-01	5.00E-01
CVFE	-1.17E-05	2.63E-05	2.87E-01	5.54E-01
DDFV-BHU	-5.814E-10	-3.35E-10	4.97E-01	5.02E-01
DDFV-HER	2.45E-10	-1.83E-10	4.80E-01	5.11E-01
DDFV-MNI	-4.37E-05	6.50E-05	5.07E-01	4.93E-01
DDFV-OMN	-6.86E-10	-4.86E-10	4.98E-01	5.02E-01
DG-C	-1.66E-07	1.41E-07	5.08E-01	4.92E-01
DG-W	5.02E-01	0.00E+00	4.98E-01	0.00E+00
FEQ1	5.51E-06	7.15E-05	5.46E-01	4.89E-01
FEQ2	-5.52E-05	1.96E-05	4.98E-01	5.01E-01
FVSYM	1.37E-04	-1.15E-04	4.96E-01	5.04E-01
FVPMMD	1.76E-06	3.5E-06	4.55E-01	5.44E-01
MFD-BLS	-5.14E-04	-3.13E-03	5.01E-01	5.03E-01
MFD-FHE	4.48E-04	-4.08E-03	5.03E-01	5.01E-01
MFD-MAR	-1.79E-02	2.61E-03	5.05E-01	5.10E-01
MFV	-2.30E-02	4.95E-02	2.74E-01	6.99E-01
NMFV	0.00E+00	0.00E+00	4.99E-01	5.01E-01
SUSHI-NP	7.35E-04	1.29E-04	4.99E-01	5.00E-01
SUSHI-P	-4.21E-02	-3.29E-02	5.38E-01	5.37E-01

Table 13. *Boundary fluxes for Test 8*

In the first line of Tables 12 and 13, we give the minimum and maximum values and the fluxes obtained with the scheme SUSHI-P for a 201×201 uniform grid which was chosen parallel to the axes. The behaviour of the corresponding approximate solution is represented in Figure 12.

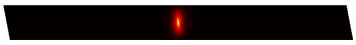

Figure 12. *Approximate solution on a fine uniform grid for Test 8*

The minimum value `umin` given by the schemes ranges from $-7.21E{-}02$ (FVSYM) to $3.26E-06$ (SUSHI-P), while the maximum value `umax` ranges from $6.77E-03$ (SUSHI-P) to $3.99E-01$ (FVPMMD).

There are only three schemes which remain positive, namely NMFV, FVPMMD and SUSHI-P. Both latter schemes, however, provide fluxes which differ from the expected fluxes (which are calculated from a fine grid discretization and given on the first line of Table 13). The only scheme which respects positive while also yielding the correct flux is NMFV, which is a nonlinear scheme. This reinforces the conjecture [**?**] that nonlinear schemes should be used if positiveness is sought, even in the case of linear problems,.

12. Test 9: anisotropy and wells [?]

Here, Ω is again the square unit domain $\Omega = (0,1) \times (0,1)$. The medium is homogeneous and anisotropic with

$$\mathbf{K} = M(-\theta) \begin{bmatrix} 1 & 0 \\ 0 & 10^{-3} \end{bmatrix} M(\theta), \qquad M(\theta) = \begin{bmatrix} \cos\theta & \sin\theta \\ -\sin\theta & \cos\theta \end{bmatrix}, \qquad [5]$$

where $\theta = 67.5°$.

The source density f is zero in all cells. Problem [1] is considered with homogeneous Neumann boundary conditions ($\Gamma_N = \partial\Omega$) on a square uniform grid `mesh9` with 11×11 cells. The pressure is fixed in two cells, approximating a sink and a source with fixed pressure:

$$\begin{aligned} u &= 0 \quad \text{in cell } (4,6), \\ u &= 1 \quad \text{in cell } (8,6). \end{aligned} \qquad [6]$$

The solution u of this problem should satisfy $u \in [0,1]$. This discrete problem could arise from a coarse discretization of a flow field with two wells, and where the pressure is given at the well, each well being represented by one grid cell. Of course, if the mesh were refined, then all the new fine cells that are included in the coarse mesh cells $(4,6)$ and $(8,6)$ should be set to 0 and 1 respectively .

However, the point here is not the convergence of the method as the mesh tends to 0, but rather its behaviour with respect to the discrete maximum principle on a coarse grid. In particular, we would like the scheme to give an approximate solution that:

1) stays between 0 and 1,

2) does not oscillate within the domain,

3) has no extremum on the outer (no-flow) boundary.

	umin	umax		umin	umax
CMPFA	-6.77E-01	1.68E+00			
CVFE	-1.16E-01	1.12E+00	FVPMMD	0.00E+00	1.00E+00
DDFV-BHU	-1.38E-01	1.14E+00	MFD-BLS	-4.30E-02	1.04E+00
DDFV-HER	-1.03E-01	1.10E+00	MFD-FHE	-4.21E-02	1.04E+00
DDFV-OMN	-7.07E-02	1.07E+00	MFD-MAR	-4.30E-02	1.04E+00
DG-C	-1.02E-03	9.98E-01	MFE	0.00E+00	1.00E+00
FEQ1	-2.36E-02	1.02E+00	MFV	-1.22E-01	1.07E+00
FEQ2	-5.94E-03	1.01E+00	NMFV	1.83E-02	1.01E+00
FVHYB	-3.69E-02	1.04E+00	SUSHI-NP	-1.00E+00	2.00E+00
FVSYM	-7.63E-02	1.07E+00	SUSHI-P	0.00E+00	1.00E+00

Table 14. *Values of umin and umax for Test 9*

0.03	0.03	0.04	0.03	0.02	0.08	0.25	0.48	0.73	0.90	0.97
0.03	0.03	0.03	0.02	0.03	0.14	0.34	0.59	0.81	0.94	0.97
0.03	0.03	0.04	0.02	0.06	0.21	0.44	0.69	0.88	0.96	0.97
0.03	0.03	0.04	0.02	0.10	0.30	0.53	0.78	0.94	0.97	0.97
0.03	0.03	0.05	0.02	0.17	0.41	0.62	0.89	0.96	0.96	0.97
0.03	0.04	0.04	0.00	0.28	0.50	0.72	1.00	0.96	0.96	0.97
0.03	0.04	0.04	0.11	0.38	0.59	0.83	0.98	0.95	0.97	0.97
0.03	0.03	0.06	0.22	0.47	0.70	0.90	0.98	0.96	0.97	0.97
0.03	0.04	0.12	0.31	0.56	0.79	0.94	0.98	0.96	0.97	0.97
0.03	0.06	0.19	0.41	0.66	0.86	0.97	0.98	0.97	0.97	0.97
0.03	0.10	0.27	0.52	0.75	0.92	0.98	0.97	0.96	0.97	0.97

Table 15. *Values given by the* MFE *scheme for Test 9*

On this test, most of the schemes which were tested violate the Hopf lemmas, as can be seen in Table 14. The SUSHI-NPscheme, although it does not show internal oscillations, has extreme values which are very much out of the bounds (-1.00 and 2.00) while the extremal values of most of the other schemes violate their bounds from less than 10 per cent. Most of the schemes for which the values are provided show oscillations of the solution. The only schemes which remain positive are the schemes FVPMMD, SUSHI-P and NMFV. This latter scheme, however, provides values which are greater than 1 (it is positive, but does not respect the discrete maximum principle) and shows some small internal oscillations. The schemes FVPMMD and SUSHI-P provide values which stay within the bounds 0 and 1, and show very little oscillations within the domain. However, the values provided by the schemes are quite different, since the values given by FVPMMD on the boundary range from roughly 0.3

to 0.6, while those given by SUSHI-P range from 0.02 to 0.98., values which are close to those given by the MFE scheme in Table 15.

13. Conclusion

This paper proposes a comparison of about 20 numerical approximations for a family of two-dimensional anisotropic diffusion problems. The nine tests presented here involve both a wide class of diffusion tensors (anisotropic and at time heterogeneous and/or discontinuous) and a wide class of (sometimes non-conforming) meshes.

A first remarkable feature of the benchmark is the relative homogeneity of the results which are obtained by the different methods. In some cases, the convergence curves are so close to one another that it is difficult to distinguish them. It is therefore difficult to rate the schemes, and we did not attempt to do so. The choice of a scheme is problem dependent. It may result from considerations on robustness (postiveness, maximum principle, etc.) and accuracy, but can also be largely influenced from other considerations such as existing codes, coupling problems or merely data structures.

As predicted by the theory, we observe that the higher order schemes FEP2, FEQ2 or DG-C feature a better order of convergence for the L^2 norm of the solution and also asymptotically for the L^2 norm of its gradient. Nevertheless, DDFV methods are able to provide particularly low errors of the gradient, which are even smaller than the higher order schemes on coarse meshes.

The robustness of the schemes with respect to the maximum principle is a great challenge. The results vary from one scheme to another, according to the meshes or to the anisotropy of the diffusion tensor. Cell centred schemes and the mimetic scheme generally seem a bit more robust than the DG or DDFV schemes. However, in more severe cases, it seems, as conjectured in [**?**], that nonlinear schemes like FVPMMD or NMFV should be used even for linear problems to ensure the positiveness of the schemes.

We expect to enrich this benchmark with other existing methods and with some other challenging problems in view to improve the existing methods or develop some new algorithms. We also hope that this benchmark will serve as a bridge between the different scheme developers: it has proven that the behaviour of the schemes is comparable on the cases which are studied here, and it would be interesting to compare them on a more mathematical basis. We finally plan to extend this benchmark to some coupling between such an anisotropic elliptic equation and a transport equation and why not to 3D anisotropic diffusion problems.

14. Acknowledgment

The present paper is a synthesis of the work of many people:

• we first warmly thank all participants for their active collaboration in this benchmark, and for letting us use their results in this synthesis,

• we are also very grateful to I. Aavatsmark, F. Boyer, R. Eymard, T. Gallouët, C. Le Potier, G. Manzini and R. Masson for their help in the benchmark design.

This work was supported by GDR MOMAS, CNRS/PACEN.

15. The meshes

We give here the figures of the families of meshes which were used here, except for the uniform square meshes. The family of meshes mesh2 is a uniform square mesh, with size ranging from 3.54E-01 (`mesh2_2`) to 5.52E-03 (`mesh2_7`). The mesh `mesh9` is a 11×11 uniform square mesh. For more details see `http://www.latp.univ-mrs.fr/fvca5/`, where the data files are also given.

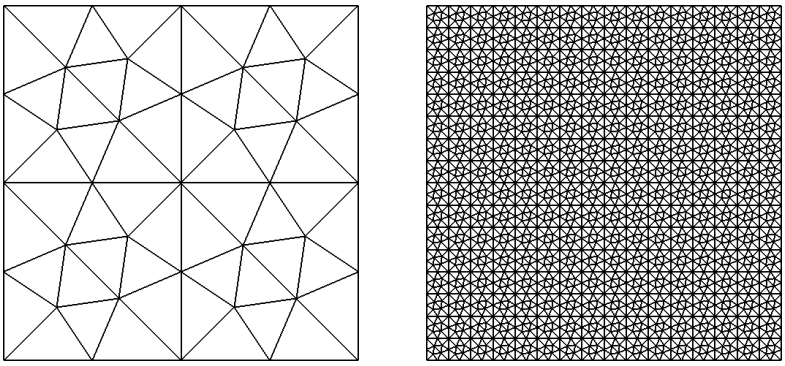

Figure 13. *Triangular mesh with acute angles: meshes* `mesh1_1` *(left) and* `mesh1_4` *(right) – Mesh size ranging from 2.50E-01 (*`mesh1_1`*) to 3.91E-03 (*`mesh1_7`*)*

16. References

[AAV 08] AAVATSMARK I., EIGESTAD G., MALLISON B., NORDBOTTEN J., "A Compact Multipoint FLux Approximation Method with Improved Robustness", *Numer Methods Partial Differential Equations*, vol. to appear, 2008.

[AFI 08] AFIF M., AMAZIANE B., "Benchmark for anisotropic problems. Numerical simulation for the anisotropic benchmark by a vertex-centred finite volume method", *these proceedings*, 2008.

[AGE 08] AGELAS L., DI PIETRO D. A., "Benchmark for anisotropic problems. A symmetric finite volume scheme for anisotropic heterogeneous second-order elliptic problems", *these proceedings*, 2008.

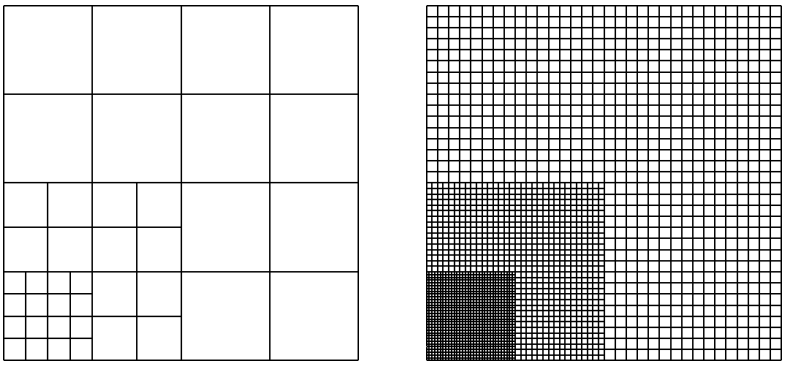

Figure 14. *Locally refined non-conforming rectangular meshes* `mesh3_1` *(left) and* `mesh3_4` *(right) – Mesh size ranging from 3.54E-01 (*`mesh3_1`*) to 2.21E-02 (*`mesh3_5`*)*

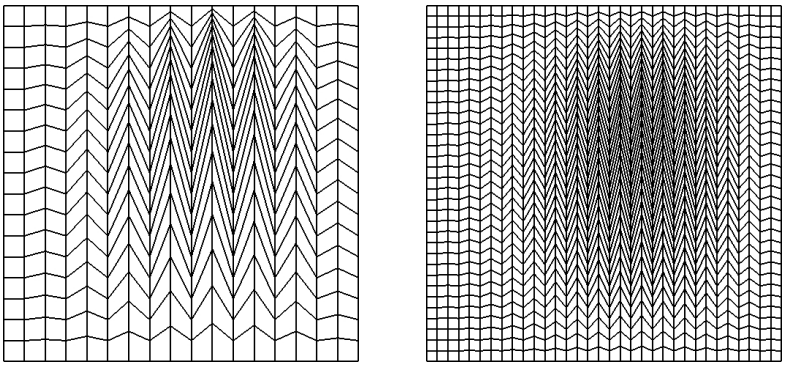

Figure 15. *Conforming distorted quadrangular mesh: meshes* `mesh4_1` *(left) and* `mesh4_2` *(right) – Mesh size 3.29E-01 (*`mesh4_1`*) and 1.70E-01 (*`mesh4_2`*)*

[AND 07] ANDREIANOV B., BOYER F., HUBERT F., "Discrete duality finite volume schemes for Leray-Lions-type elliptic problems on general 2D meshes", *Numer. Methods Partial Differential Equations*, vol. 23, num. 1, 2007, p. 145–195.

[ANS 08] ANSANAY-ALEX G., PIAR B., VOLA D., "Benchmark for anisotropic problems. Galerkin Finite Element Solution", *these proceedings*, 2008.

[BAB 92] BABUŠKA I., SURI M., "On locking and robustness in the finite element method", *SIAM J. Numer. Anal.*, vol. 29, num. 5, 1992, p. 1261–1293, Society for Industrial and Applied Mathematics.

[BOY 08] BOYER F., HUBERT F., "Benchmark for anisotropic problems. The DDFV "discrete duality finite volumes" and m-DDFV schemes", *these proceedings*, 2008.

[CHA 08] CHAINAIS-HILLAIRET C., DRONIOU J., EYMARD R., "Benchmark for anisotropic problems. Use of the mixed finite volume method", *these proceedings*, 2008.

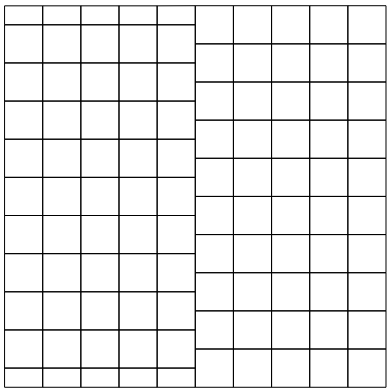

Figure 16. *Non-conforming regular rectangular mesh* `mesh5` *– Mesh size 1.41E-01*

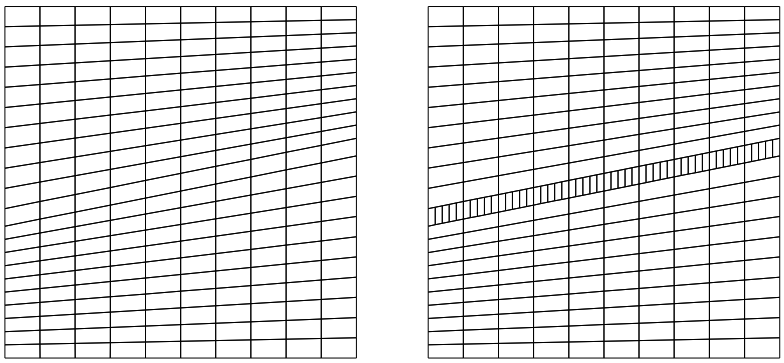

Figure 17. *Coarse oblique mesh:* `mesh6` *(Left). Fine oblique mesh for the oblique barrier and drain tests:* `mesh7` *(Right) – Mesh size 1.25E-01*

[DED 08] DEDNER A., KLÖFKORN R., "Benchmark for anisotropic problems. The Compact Discontinuous Galerkin Method for Elliptic Problems", *these proceedings*, 2008.

[DIP 08] DI PIETRO D., ERN A., "Benchmark for anisotropic problems. A discontinuous Galerkin flux for anisotropic heteroge- neous second-order elliptic problems", *these proceedings*, 2008.

[DUB 08] DUBOIS F., LALLEMAND P., TEKITEK M. M., "Benchmark for anisotropic problems. Using Lattice Boltzmann scheme for anisotropic diffusion problems", *these proceedings*, 2008.

[EYM 08] EYMARD R., GALLOUËT T., HERBIN R., "Benchmark for anisotropic problems. SUSHI: A Scheme Using Stabilization and Hybrid Interfaces for anisotropic heterogeneous diffusion problems", *these proceedings*, 2008.

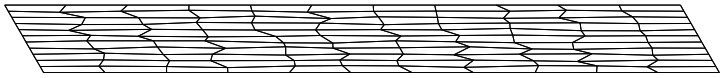

Figure 18. *Perturbed parallelogram grid* `mesh8` *with* 11×11 *cells – Mesh size 1.24E-01. To visualize the grid, on this picture the height is 3 times the real height of the grid described in the test case*

[FLE 08] FLEMISCH B., HELMIG R., "Benchmark for anisotropic problems. Numerical investigation of a mimetic finite difference method", *these proceedings*, 2008.

[GAL 07] GALLOUËT T., "Nonlinear methods for linear equations", ALIZIANE T., LEMAET K., MOKRANE A., TENIOU E., Eds., *Actes du 3-ème colloque sur les Tendances des Applications Mathématiques en Tunise, Algérie et Maroc, Tipaza, 14-18 Avril 2007*, AMNEDP-USTHB, 2007, p. 17-22, `http://www.cmi.univ-mrs.fr/~gallouet`.

[HER 08] HERMELINE F., "Benchmark for anisotropic problems. Numerical experiments with the DDFV method", *these proceedings*, 2008.

[LEP 05] LE POTIER C., "Schémas volumes finis pour des opérateurs de diffusion fortement anisotropes sur des maillages non structurés", *C. R. Math. Acad. Sci. Paris*, vol. 340, num. 12, 2005, p. 921–926.

[LEP 08] LE POTIER C., "Benchmark for anisotropic problems. Numerical results with two cell-centered finite volume schemes for heteregeneous anisotropic diffusion operators", *these proceedings*, 2008.

[LIP 08] LIPNIKOV. K., "Benchmark for anisotropic problems. Mimetic finite difference method", *these proceedings*, 2008.

[MAN 07] MANZINI G., PUTTI M., "Mesh locking effects in the finite volume solution of 2-D anisotropic diffusion equations", *J. Comput. Phys.*, vol. 220, num. 2, 2007, p. 751–771, Academic Press Professional, Inc.

[MAN 08] MANZINI G., "Benchmark for anisotropic problems. The Mimetic Finite Difference Method", *these proceedings*, 2008.

[MAR 08] MARNACH S., "Benchmark for anisotropic problems. A Mimetic Finite Difference Method", *these proceedings*, 2008.

[MOU 08] MOUKOUOP NGUENA I., NJIFENJOU A., "Benchmark for anisotropic problems. Some MPFA methods of DDFV type", *these proceedings*, 2008.

[MUN 08] MUNDAL S., DI PIETRO D. A., AAVATSMARK I., "Benchmark for anisotropic problems. Compact-stencil MPFA Method for heterogeneous highly anisotropic second-order elliptic problems", *these proceedings*, 2008.

[OMN 08] OMNES P., "Benchmark for anisotropic problems. Tests with the Discrete Duality Finite Volume method", *these proceedings*, 2008.

[SVY 08] SVYATSKIY D., "Benchmark for anisotropic problems. Nonlinear monotone finite volume method", *these proceedings*, 2008.